

Effects of Rolling-Sliding Frictions in Granular Flow Dynamics

Shunying Ji¹ Shanshan Sun¹ Ying Yan²

1. State Key Laboratory of Structural Analysis for Industrial Equipment, Dalian University of Technology, Dalian 116023, China

2. School of Traffic and Transportation, Dalian Jiaotong University, Dalian, 116028, China

Abstract Besides the sliding friction, the rolling resistance is also quite important to the dynamics of granular materials, and has been attracted people's great interests in the last decade. Recently, couple various models have been established based on linear or non-linear contact models for granular materials. The motion of particles can appear as sliding or rolling status under various normal/shear loads, roughness of particle surface and particle shape. To study the influences of sliding-rolling frictions on granular flow dynamics, the DEM code was programmed to investigate the dynamical process of particles under different scales with numerical simulations. The motion of one particle on inclined plane was simulated at micro-scale with various sliding friction coefficients and rolling friction coefficients. Moreover, the angle of repose was tested at macro-scale to analyze the influences of sliding and rolling frictions on granular materials. With these present studies, the roles of rolling and sliding frictions were understood well to analyze the dynamic characteristics and to improve the discrete element model of granular materials.

Keywords: granular materials, discrete element model, rolling friction, sliding friction, micro-macro scale.

1. Introduction

Granular flow modeling began with the 1773 paper by Coulomb who first described the yielding of granular materials as a frictional process (Campbell, 2006). In the numerical simulation of granular flow dynamics, the conventional discrete element model (DEM) has been established in two-dimension and with linear contact force model (Cundall and Strack, 1979). After that, the non-linear model was introduced even in three-dimension. In the previous discrete element models, the normal visco-elastic contact model with a Coulomb sliding friction law were most commonly applied.

For the rolling friction between particles, Ting et al. (1989) found the particle rotation can produce more realistic internal friction and bulk shear modulus for a 2-D granular material. Contact models considering rolling friction between particles have been proposed by Sakaguchi et al. (1993) and Iwashita and Oda (1998, 2000). With the MDEM (modified DEM), Iwashita and Oda(1998, 2000) studied the biaxial compression tests of granular materials and got the local strain and stress well. Based on the MDEM, other works were also carried out (Zhou et al. 1999, 2001; Jiang et al., 2005). In the studies of Zhou et al. (1999, 2001), the angle of repose was simulated for granular materials with uniform size of particles in 3D. In their studies, they did not consider the damping in rolling friction model. Recently, Jiang at el. (2005) discussed the MDEM in details and improved it well.

At the same time, some people took their efforts on the non-linear contact force models. A complete non-linear rolling friction model, which only considered the elastic contact model, was described by by Johnson (1985). Meanwhile, the viscous non-linear models were investigated by Brilliantov and Poschel (1998) and Poschel (1999). They studied the rolling friction of a viscous sphere on a hard plane and the rolling friction of a hard

cylinder on a viscous plane, respectively. In their studies, the rolling friction is only relative to the viscous portion, but is independent of the elastic deformation. The non-linear models of rolling friction above are only limited in the discussion at analytical level.

In the dynamic flow of granular materials, the sliding and rolling frictions are coupled at micro-scale (particle scale), and dominate the dynamic properties of granular system at macro-scale. Even for a very simple case, a regular particle, which is given a certain initial translational velocity and rotational velocity, can appear in pure sliding, pure rolling or sliding-rolling movement, which is controlled with the plate roughness and the initial velocity. If we consider the dynamical process of a granular system, the sliding-rolling will be coupled more complexly.

In the previous studies on the granular flow dynamics, few people paid their attentions on the coupling of sliding-rolling frictions. To understand the dynamical characteristics of granular materials well, the movement of a single particle on a horizontal and sloped plated will be studied at micro-scale, while the angle of repose and the rotation in a shear cell will be simulated at macro-scale to investigate the influences of sliding-rolling frictions in this study.

2. Sliding and Rolling Frictions in Contact Model of Particles

In the conventional DEM, each contact is replaced by a set of spring, dash pots, no-tension joints, and a shear slider. Based on it, the MDEM of Iwashita and Oda(1998, 2000) considers the rolling resistance between particles. The whole contact force model with rolling friction is as shown in Fig. 1. For the stiffness and damping in normal and tangential directions, a serious contact force model, which can be linear or non-linear, appeared in literatures (Coundal et al., 1979; Ji et al., 2006, 2008). Here, the sliding and rolling force model will be considered well.

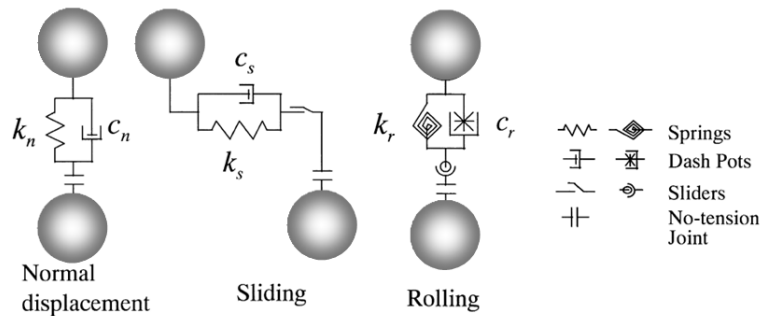


Fig. 1. The contact model of EDEM (Iwashita K and Oda M, 1998, 2000)

Adopting the linear contact model based on the Mohr-Coulomb friction law and the rolling friction of MDEM, the magnitudes of shear force and rolling resistant moment can be written as

$$F_s = \min(K_s x_s + C_s \dot{x}_s, \mu_c F_n) \quad (1)$$

$$M_r = \min(K_r \theta + C_r \dot{\theta}, \mu_r F_n) \quad (2)$$

where K_s is the tangential stiffness, C_s is the tangential damping coefficients, μ_c is the friction coefficient, x_s is tangential displacement; K_r is the rolling stiffness, C_r is the viscosity coefficient for rolling motion, θ is the

relative particle rotation, η is the coefficient of rolling friction.

In the granular flow dynamics, the mechanism of sliding friction has been understood well, but that of rolling friction was known less. Basically as we know, the sliding friction is induced with the elastic deformation of particles, which is shown in Fig. 2(a). With rolling friction, the additional torque under particle's elastic deformation can be considered to model the particle rotation more accurately.

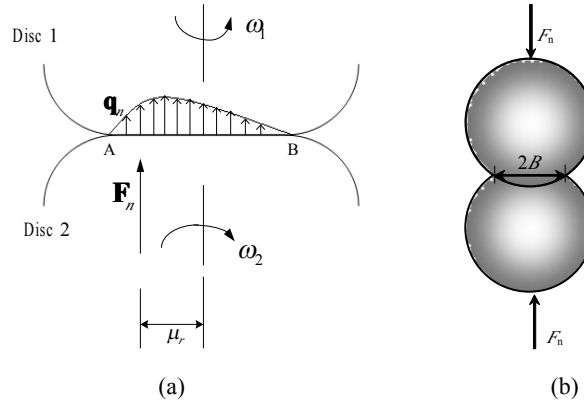


Fig. 2. Normal traction distribution exerted on particle to induce rolling friction

For the linear contact force model, the rolling stiffness and rolling friction coefficient are set as (Iwashita K and Oda M, 1998, 2000)

$$K_r = K_s R^2, \quad \mu_r = \zeta B \quad (3)$$

Recently, Jiang et al. (2005) got the following parameters based on their understanding as

$$K_r = \frac{K_n B^2}{12}, \quad \mu_r = B/6 \quad (4)$$

where R is the radius of particle, B is half of the diameter of the contact area, as shown in Fig. 2(b), ζ is a non-dimensional rolling friction parameter, and was set as 0.0, 1.0 or 5.0 (Iwashita and Oda, 1998, 2000). The rolling viscous coefficient C_r was set as a constant in the studies of Iwashita and Oda (1998, 2000), but in Jiang et al. (2005) it was set as

$$C_r = \frac{C_n B^2}{12} \quad (5)$$

where C_n is the normal damping coefficient.

Combining the rolling friction models of Iwashita and Oda (1998, 2000) and Jiang et al., (2006), the parameters are given here as

$$K_r = \zeta K_s R^2, \quad C_r = \frac{C_n B^2}{12}, \quad \mu_r = \zeta B \quad (6)$$

From the rolling stiffness K_r and rolling friction coefficient μ_r above, both of them are proportional to the parameter ζ . In the modeling of shear force, the tangential stiffness K_s is set a constant usually, while the sliding friction coefficient μ_c can be various under different boundary or particle roughness. The sliding and rolling frictions are given in Fig.3, where α and β are two given numbers to define the magnitudes of sliding and rolling frictions.

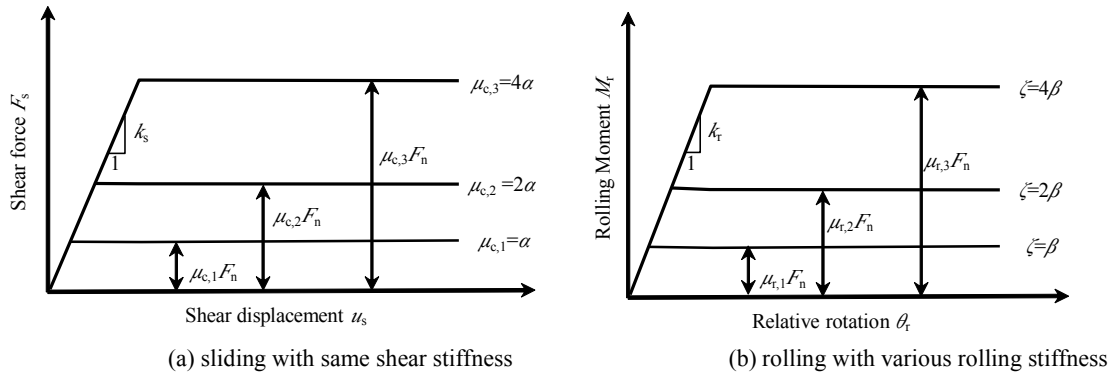


Fig. 3. Sliding and rolling contacts models at contact points. (a) sliding; (b) rolling

3. Sliding-Rolling of Single Particle on horizontal and incline Planes at Micro-Scale

To understand the influences of sliding and rolling frictions of particles, the motions of single particle on a horizontal and incline planes are simulated, respectively. Based on the simulated results, the conditions for pure sliding, pure rolling, even the transition of the two movements are discussed in details.

3.1 Motion on horizontal plane

In this case, one regular particle is put on a horizontal plane with the initial translational velocity u_0 and rotation velocity ω_0 (shown as Fig. 4). With various initial velocities, and also considering the sliding and rolling friction coefficients, the movements of this particle will be different. Here, two special cases will be tested with pure initial translation movement with $\omega_0 = 0.0 \text{ s}^{-1}$ and pure initial rotation movement with $u_0 = 0.0 \text{ m/s}$. Some computational parameters are listed in Table 1.

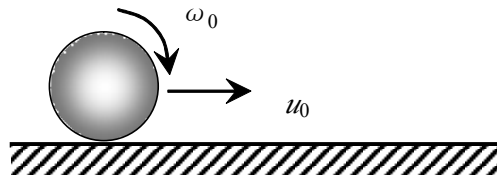

 Fig. 4. Motion of single particle on a horizontal plane with initial velocity u_0 and ω_0

Table 1. Major parameters for single particle movement on horizontal plane

Definitions	Symbol	Values	Definitions	Symbol	Values
Particle diameter	D	1 cm	Normal stiffness	K_n	10^5 N/m
Particle density	ρ	2600 kg/m^3	Restitution coefficient	e	0.8
Sliding friction coefficient	μ_c	0.0, 0.1, 0.5	Initial translational velocity	u_0	0.0, 0.5 m/s
Rolling friction parameter	ζ	0.0, 2.0, 5.0	Initial rotational velocity	ω_0	100, 0.0 s^{-1}

A series of tests are constructed with various sliding friction coefficients, rolling friction coefficients and initial velocities to study the influence of sliding and rolling frictions on the movement of single particle on a horizontal plane. In Figs. 5 and 6, we plotted the two cases of initial pure translational movement and pure rotational movement at the start stage.

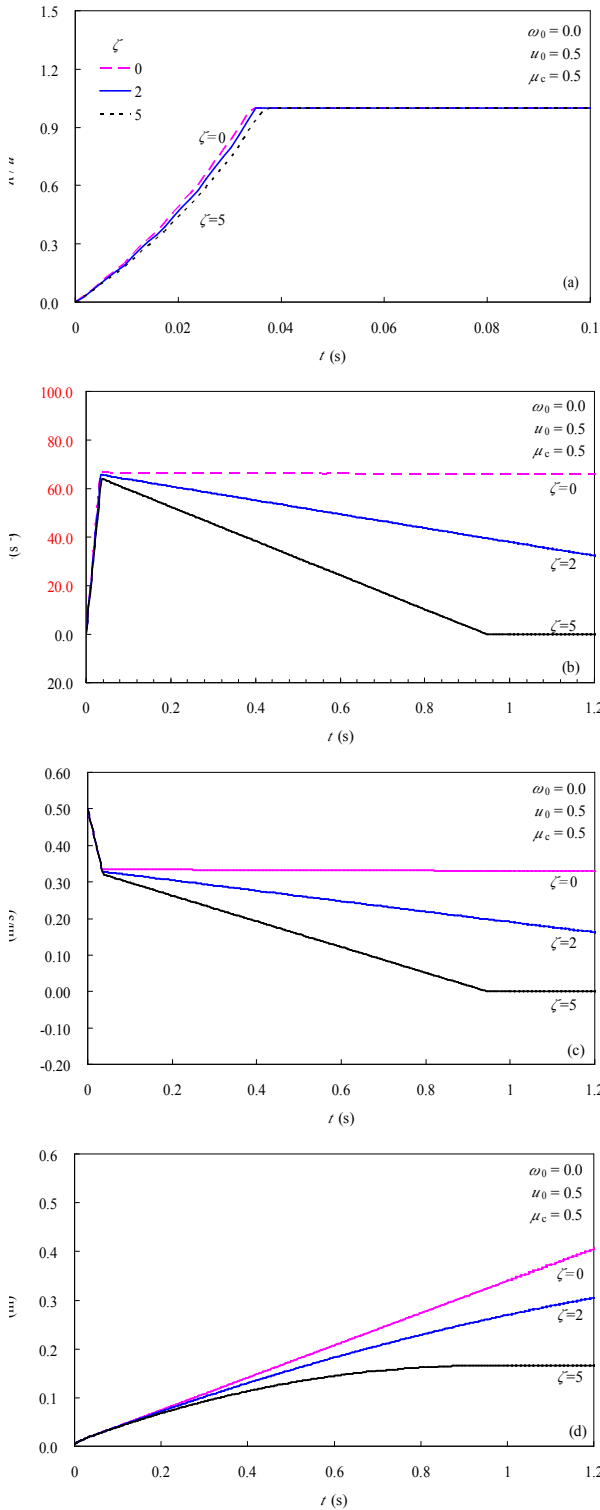


Fig. 5. Simulated results for initial rotational velocity $\omega_0 = 0.0 \text{ s}^{-1}$, and initial translational velocity $u_0 = 0.5 \text{ m/s}$ (pure initial rotation).

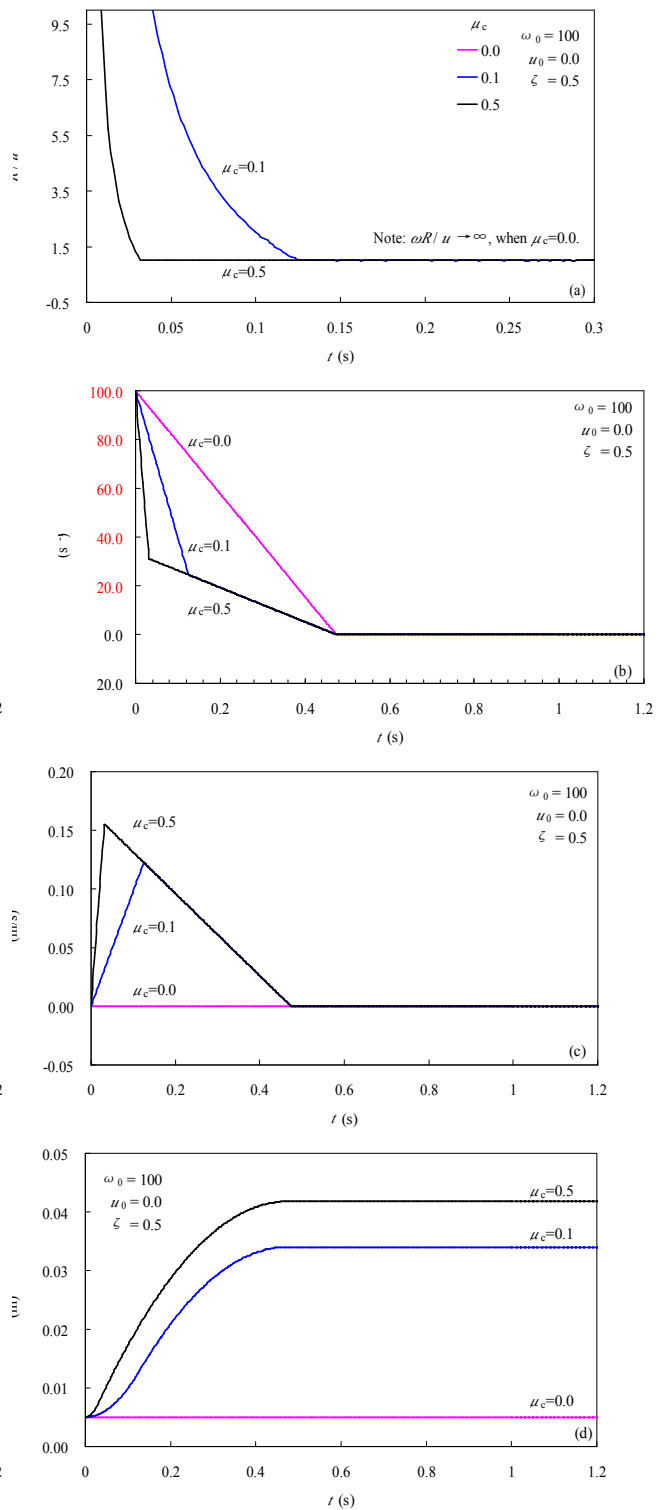


Fig. 6. Simulated results for initial rotational velocity $\omega_0 = 100 \text{ s}^{-1}$ and initial translational velocity $u_0 = 0.50 \text{ m/s}$ (pure initial translation).

For the initial pure translational case (as Fig. 5), we can find the movement of particle can be separated into three stages: sliding, rolling and static. In the first stage of sliding, the rotation velocity ω increases from zero to 65 s^{-1} at the time around 0.04 s under the action of boundary sliding friction, while the translational velocity u decreases from 0.50 m/s to 0.32 m/s (as Fig. 5(b) and (c)). In this stage, the influences of sliding friction has less

influences on the movement of particle, since the friction supplied enough shear force to increase the rotation velocity. In the second stage of rotation, all of the rotational and translational velocities decrease and approach to zero. The three stages is complete when $\zeta = 5.0$ in this simulation. With larger ζ , the decreasing rate is larger since more kinetic energy of particle was dissipated in the rolling. When all of the kinetic energy is dissipated over, the rotation velocity and translational velocity approach zero finally. In other words, the movement of particle goes into the third stage of static. But for the case of $\zeta = 0.0$, which means the rolling friction is ignored, the rotational and translational velocities keep constant. This really is a bizarre phenomenon since the particle will keep rotation forever, which is impossible in the real world. Therefore, the rotation friction must be considered in the numerical simulation of particles. From Fig. 5(a), we can find the dimensionless rotation velocity $\omega R/u$ increase from zero to 1.0 in the first stage of sliding, keep as constant 1.0 in the second stage of rotation, then goes into the static stage if ζ is not zero. In Fig. 5(d), the motional displacements of the particle can be linear or non-linear curves which can be explained with the particle velocities. Especially for the case of $\zeta = 0.0$, the displacement increase with time and can be infinity, while other curves of $\zeta = 0.2$ or 5.0 will go to a constant values when the particle goes into the static stage.

For the initial pure rotational case (as Fig. 6), the motions of this particle can also be separated into three stages: sliding, rolling and static. In fact, in the first stage of sliding, the particle motion is mainly dominated by the sliding friction between particle and boundary, but the rotation friction appears also. Similar to the first case of initial pure translation in Fig. 5, we can understand the motion characteristics in Fig. 6 well. But for the complete smooth situation of $\mu_c = 0.0$, the translational velocity keeps zero without the sliding friction, but the rotation velocity still decreases under the action of rolling friction. From the simulated results of single particle motion on horizontal plane (as Figs. 5, 6), we can find the particle motion is affected with the rolling and sliding frictions obviously.

3.2 Motion on inclined plane

To understand the sliding-rolling friction further, we set one static single particle on one side of a horizontal plane, then lift this side slowly to make an inclined plane (shown as Fig. 7). For this case, we can image the motion of particle will be rolling or sliding under various conditions. In the following, the analytical solutions and the numerical results will be investigated to determine the influences of sliding and rolling frictions.

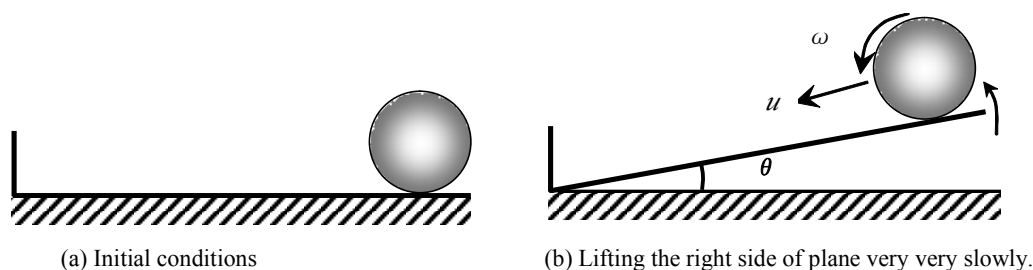


Fig. 7. Motion of single particle on an inclined plane with initial velocity u_0 and ω_0

(1) Analytical solution

For the inclined plane with slope θ and the particle weight G , the normal and tangential force components can be written as

$$F_t = G \sin \theta , \quad F_n = G \cos \theta \quad (7)$$

If the particle starts to slide or roll on the inclined plane, the maximum sliding force F_s and rolling friction

moment M can be written as

$$F_s = \mu_c F_n, \quad M_r = \zeta B F_n = \mu_r F_n \quad (8)$$

where the half of the contact length B can be written as

$$B = \sqrt{R^2 - (R - \delta)^2} \approx \sqrt{2R\delta} = \sqrt{2RF_n / K_n} \quad (9)$$

For the particle motion, the sliding-rolling conditions can be written as

$$\begin{cases} F_t > F_s, & F_t R < M_r & \text{sliding} \\ F_t < F_s, & F_t R > M_r & \text{rolling} \\ \text{static} & & \text{otherwise} \end{cases} \quad (10)$$

For the rolling situation, the conditions can be written as

$$\frac{\sin^2 \theta}{\cos^3 \theta} > \frac{2\zeta^2 G}{RK_n} \quad \text{and} \quad \tan \theta < \mu_c \quad (11)$$

Similar, the conditions for sliding situation can be determined.

(2) Numerical solution

To validate the analytical solution above, the motion of single particle on inclined plane is simulated with DEM. Here, setting the particle diameter $D = 6\text{mm}$, the normal stiffness $K_n = 6 \times 10^4 \text{ N/m}$, the sliding friction coefficient μ_c is from 0.0 to 0.6, the rolling friction parameter ζ is from 0 to 6.0. The other parameters are listed in Table 1.

In the DEM simulation, we put one particle on one side of the horizontal plane, then lift this side slowly with rotation velocity $1.0 \times 10^{-6} \text{ s}^{-1}$. When the plane rotates to a certain angle θ , the particle will move down. With different sliding friction coefficient μ_c and rolling friction parameter ζ , the particle will perform as sliding or rolling.

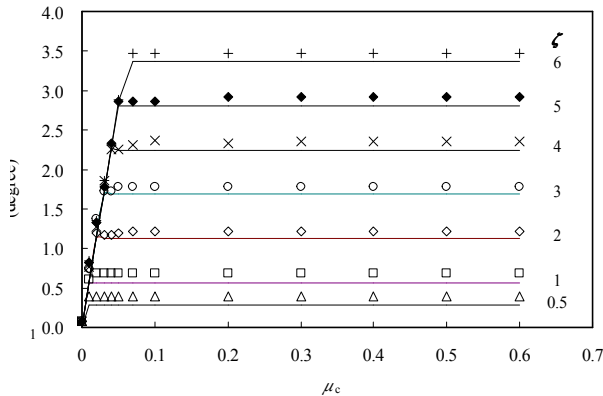


Fig. 8. Slope of the inclined plane for particle motion

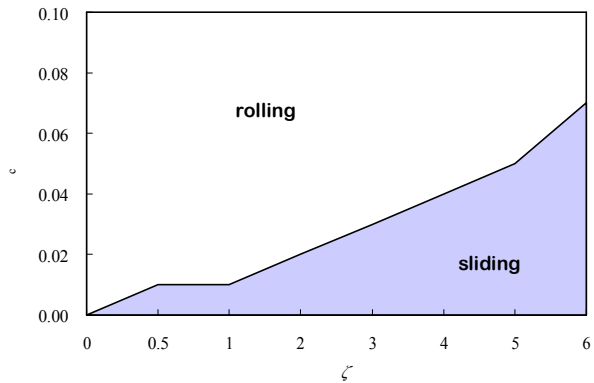


Fig. 9. Sliding and rolling zones for particle motion

Under various sliding friction coefficients and rolling friction parameters, the minimum angles of the plane for particle moving down are plotted in Fig. 8, where the analytical solution is also plotted to compare with the numerical results. With the increase of sliding friction coefficient for smaller μ_c , the angle of inclined plane increase accordingly. Under this condition, the particle performs as sliding motion, which depends on the value of μ_c . For larger μ_c , the motion of particle performs as rolling, and is dominated by the rolling friction parameter ζ . To show the sliding or rolling motion obviously, a divisional curve is plotted in Fig. 9. Based on the analytical and numerical results for particle sliding-rolling motions, we can find the particle performs as sliding or rolling motions under smaller or larger sliding frictions, respectively.

4. Influences of Sliding-Rolling Frictions on Granular Flow Dynamics at Macro-Scale

With the analysis of single particle motions at micro-scale, we learned some influences of sliding-rolling friction on particle motions. In this section, we study the granular dynamical behaviors with two numerical cases at micro-scale. One is on the angle of repose, the other is the test of rotating annular shear cell.

4.1 Angle of repose

The angle of repose is a basic physical property of granular materials, and has been investigated with both of numerical approaches and physical tests already (Zhou et al., 1999, 2001; Suiker et al., 2004; Staron et al. 2005). Here, we analyze the influences of the sliding friction coefficient μ_c and the rolling friction parameter ζ on the granular dynamics with the angle of repose. In this 2D DEM simulation, the process to generate the angle of repose is shown in Fig. 10, where the structure size is also given. The particle diameter has a uniform probability distribution in $[0.9D, 1.0D]$. The basic parameters are listed in Table 2, and others are selected in Table 1.

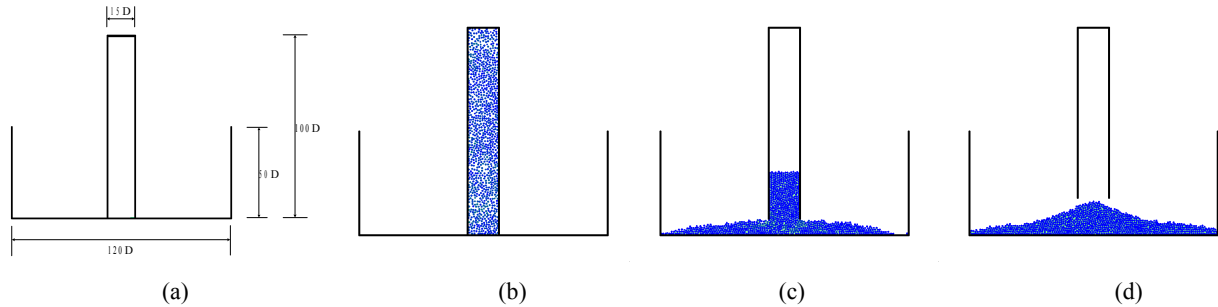


Fig. 10. Geometry of the structure and the collapsing process. Here D is the averaged particle diameter.

Table 2. Major parameters for angle of repose DEM simulation

Definitions	Symbol	Values	Definitions	Symbol	Values
Averaged particle diameter	D	1 mm	Normal stiffness	K_n	1.5 MN/m
Total particle number	N	973	Sliding friction with side wall	μ_{c_sw}	0.0
Sliding friction coefficient	μ_c	0.0 - 2.0	Sliding friction with bottom wall	μ_{c_bw}	1.0
Rolling friction parameter	ζ	0.0, 2.0, 8.0	Lifting velocity of center cylinder	u_c	2.0 mm/s

In the DEM simulation for angle of repose generation, the particles are filled in the center closed cylinder randomly, then are deposited down under the action of gravities. When the particle system goes into static state, the center cylinder is lifted slowly enough with the velocity 2.0 mm/s. To overcome the influences of sidewall friction, all of the sliding friction coefficients are set as zero, while the bottom boundary is set to 1.0 to supply enough friction force. With the lifting of cylinder, the particles flow out slowly to generate a heap. In the simulation, there are two static states of the particle systems. The first one is for the initial condition before center cylinder lifting, the second one is to obtain the angle of repose after lifting. Here we define a variable E_k , which is the total kinetic energy of the particle system, to determine the static state when it approaches zero. After the collapse of the granular pile, the angle of repose can be determined with the method shown in Fig. 11. With various sliding and rolling friction parameters, the angles of repose are quite different. With the parameters listed in Table 2, the angles of repose are obtained and plotted in Fig. 12.

From the simulated results in Fig. 12, we can find the angle of repose is affected with the sliding friction and rolling friction together. When the rolling friction parameter ζ is fixed, the angle of repose can increase with the

increase of the sliding friction μ_c when $\mu_c < 0.5$, but keep around a constant value when $\mu_c > 0.5$. This means the angle of repose can not increase if only increase the roughness of particle surface. In other words, if the sliding friction coefficient μ_c is large enough, such as $\mu_c > 0.5$ in this case, the particle will move as rolling style. When the rolling parameter ζ is keep as a constant, the particle will roll down the granular pile to keep the angle of repose in a steady number. If keeping the sliding friction coefficient μ_c as a constant, the angle of repose has a similar relationship with the rolling parameter ζ . Therefore, the angle of repose θ is dominated with the sliding and rolling frictions together. Only increase any variable of μ_c and ζ , θ can increase at beginning, then approach a fixed value, which is determined with the other variable of μ_c and ζ .

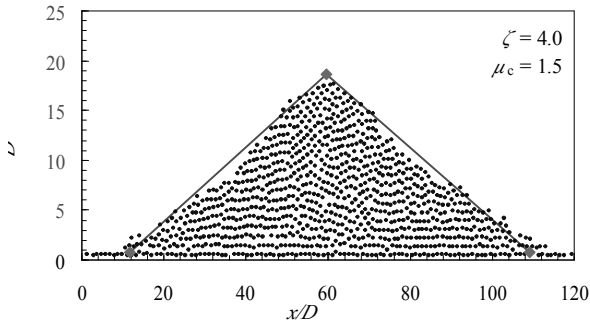


Fig. 11. Determination of angle of repose for the case of $\mu_c = 1.5$, $\zeta = 4.0$.

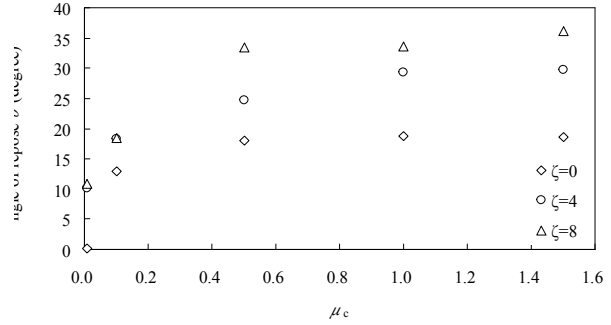


Fig. 12 Distribution of angle of repose under various friction coefficients.

4.2 Shear force in annular shear cell

The annular shear cell test is a classic method to determine the mechanical properties of granular materials, and has been studied widely (e.g. Savage and Sayed, 1984; Hanes and Inman, 1985; Hsiau et al., 1998; Qin, 2000). Bagnold (1954) constructed this physical experiment firstly, and determined the famous ‘‘Bagnold Scale’’ for granular materials. In this study, we use an annular shear cell to establish the comparison between the physical and DE simulation results. The physical experiment apparatus were described by Qin (2000), and the glass particles were selected in the physical experiments.

The particles were placed in a numerically defined shear cell with the same dimensions as used in the physical experiment. For the boundary conditions, we used a radial hexagonal packing to produce the top and bottom surfaces. To reduce the simulation time, we only simulated the shear cell of 30° , and the hoop boundary was deal with periodic conditions (shown as in Fig. 13). In the tests, the normal stress was applied on the top cover, and the bottom cover was given a rotating velocity. The interior and exterior cylinders rotate with the bottom cover together. In the physical and numerical experiments, the torques acting on the top cover are measured. The computational parameters are listed in Table 3.

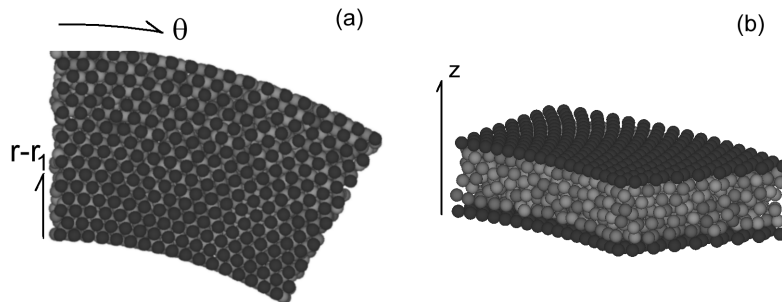


Fig. 13. The (a) boundary and (b) interior packing of a simulated 30° shear cell. In which r_1 is the radius of the inner circle.

Table 3. Parameters used in the DEM simulations of shear cell tests.

Definitions	Symbol	values	Definitions	Symbol	values
Mean particle diameter	D	3 mm	Total mass of shear material	M	0.675 kg
Boundary particle diameter	D_b	3 mm	Sphere-sphere restitution coefficient	e_{p-p}	0.972
Outside radius of shear cell	r_2	146 mm	Sphere-wall restitution coefficient	e_{p-w}	0.97
Inside radius of shear cell	r_1	102 mm	Height of the shear cell	H	12.11-16.66 mm
Particle density	ρ	2946 kg/m ³	Normal stiffness	K_n	20 kN/m
Rotation speed	n	2 -170 RPM	Normal stress	σ_{zz}	0.6 - 2.1 kPa

Under different normal stresses and rotation velocities, and setting the sliding friction coefficient $\mu_c = 0.177$ and $\zeta = 0.0$, the simulated torques acting on the top cover are plotted in Fig. 14 (a). We can find the simulated torques are about half of that of physical results. To increase the simulated torques, we considered the rolling friction and setting $\zeta = 3.0$, and the simulated results were improved, shown as Fig. 14(b). But the numerical results can not match the physical data well. Even we increased the rolling friction parameter ζ a lots, the simulated torque can not increase obviously. At this time, we should consider the combination of the sliding and rolling friction.

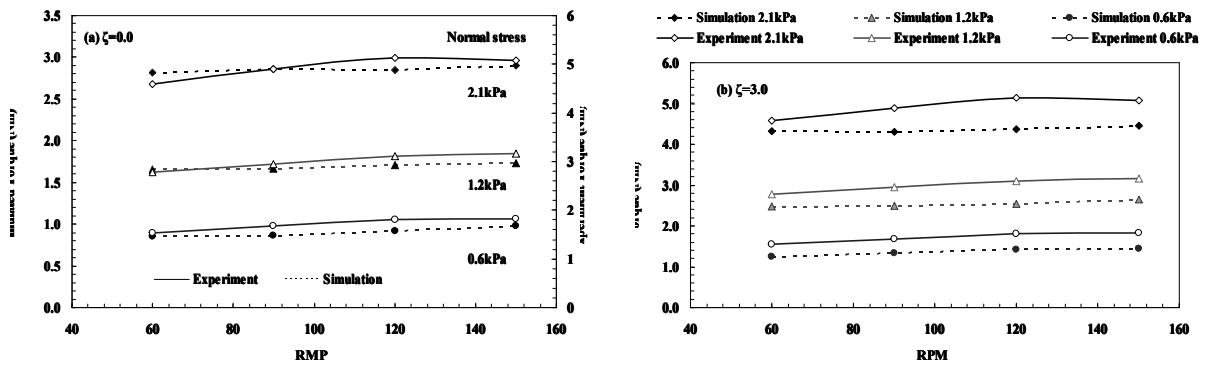


Fig. 14. Numerical results of glass particles in the shear cell. (a) without rolling friction; (b) with rolling friction.

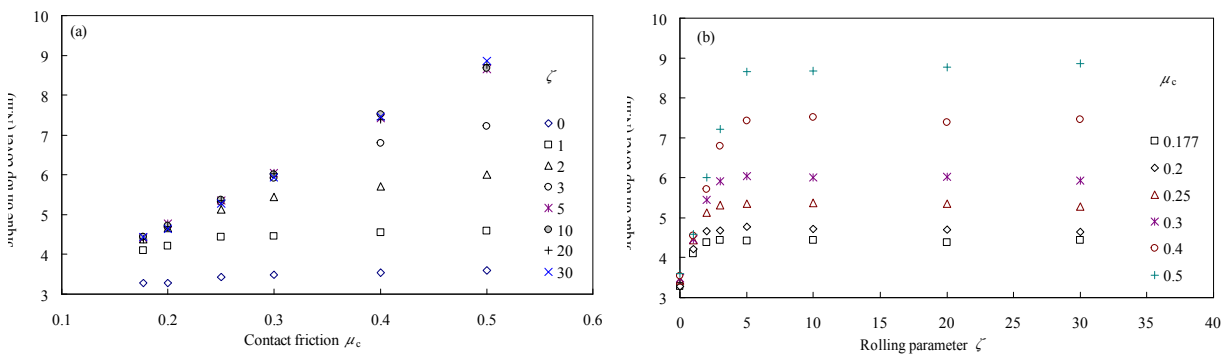


Fig. 15. Combined effect of sliding and rolling friction on the resisting torque.

Here we only select one case with glass particles under 2.1kN of normal load and 150RPM rotation. The simulated torques were plotted in Fig. 15. When the rolling friction is zero, increasing the sliding friction from 0.177 to 0.5 only increased the resisting torque from 3.28 to 3.60. But when $\zeta = 5.0$, the increase between $\mu_c = 0.177$ and 0.5 is significant, from 4.42 to 8.66. Similar to sliding friction, the effect of rolling friction also approaches an asymptote at large values of ζ . Fig. 16 shows the combination of sliding and rolling friction,

assuming both remain constant, for the full range of normal load and shearing rate as tested in the glass particle case shown in Fig. 14. In this case, we set $\mu_c = 0.25$ and $\zeta = 3.0$, and all other parameters are identical as given in Table 3. The comparison between the experimental and the simulated results is much improved.

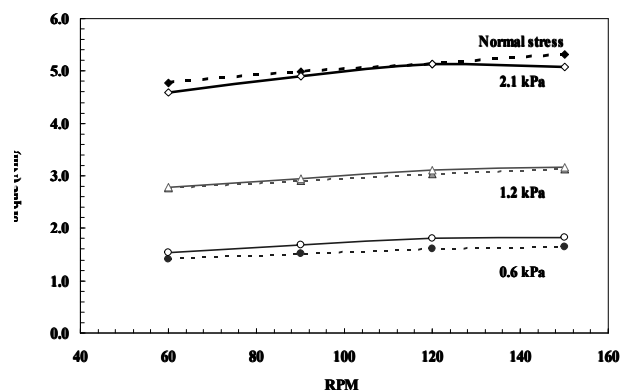


Fig. 16. Comparisons of physical test results with simulated data with $\mu_c = 0.25$, $\zeta = 3.0$ and other parameters identical to the case shown in Fig. 14. Solid lines are from the experiment and dashed lines are from simulations.

5. Conclusions

In the granular flow dynamics, the rolling friction between particles is same important as that of sliding friction, but people pay less attention on the mechanism of rolling friction. In this study, the influence of rolling friction on the dynamic properties of granular materials was investigated. As the computational model of sliding friction coefficient μ_c , the rolling friction can also be defined with the rolling friction coefficient μ_r . But different to the influence of roughness on μ_c , μ_r is dominated with the elastic deformation of particle. To define the rolling friction coefficient μ_r , a rolling parameter ζ is introduced.

With the single particle motion at micro-scale and the dynamic properties of granular system, the influences of sliding and rolling frictions were investigated with various sliding friction coefficient μ_c and the rolling friction parameter ζ . At the micro-scale, the motions of single particle on a horizontal and a inclined planes were tested. At the macro-scale, the angle of repose for granular pile and the torque acting on the annular shear cell were simulated. Based on all of the simulated results above, the properties of granular flow are affected by the combination of sliding and rolling frictions. For large roughness of particle or boundary is large enough, i.e. high μ_c , the particles perform in rolling behaviors. While for large rolling frictions, i.e. high ζ , the particles perform in sliding behaviors easier.

The influence of rolling friction on the granular flow dynamics was analyzed in this study, but the mechanism of rolling friction is still an open problem. For the regular particles, the elastic deformation is the main reason to generate the rolling resistance. But for the irregular particle, the influence of particle shape is more obvious. Physical experiments and numerical simulations will be adopted to understand the rolling friction for irregular particles in the future works.

References

1. Brilliantov N V, Poschel T. Rolling friction of a viscous sphere on a hard plane. *Europhysics Letters*, 1998, 42(5):511-516.
2. Campbell C S. Granular material flows - An overview. *Powder Technology*, 2006, 162:208-229.

3. Cundall P A and Strack O D L. A discrete numerical model for granular assemblies. *Geotechnique*, 1979, 29(1): 47-65.
4. Hanes D M, Inman D L. Observations of rapidly flowing granular fluid mixtures. *Journal of Fluid Mechanics*, 1985, 150: 357-380.
5. Hsiau S, Jang H. Measurements of velocity fluctuations of granular materials in a shear cell. *Experimental Thermal and Fluid Science*, 1998, 17: 202-209.
6. Iwashita K, Oda M. Micro-deformation mechanism of shear banding process based on modified distinct element method. *Powder Technology*, 2000, 109:192-205.
7. Iwashita K, Oda M. Rolling resistance at contacts in simulation of shear band development by DE. *Journal of Engineering Mechanics*, 1998, 124(3):285-292.
8. Shunying Ji, Hayley H Shen. Effect of Contact Force Models on Granular Flow Dynamics. *ASCE Journal of Engineering Mechanics*, 2006, 132(11): 1252-1259.
9. Ji S, Shen H H. Internal parameters and regime map for soft polydispersed granular materials. *Journal of Rheology*, 2008, 52(1): 87-103.
10. Jiang M J, Yu H-S, Harris D. A novel discrete model for granular material incorporating rolling resistance. *Computers and Geotechnics*, 2005, 32:340-357.
11. Oda M, Iwashita K. Study on couple stress and shear band development in granular media based on numerical simulation analyses. *International Journal of Engineering Science*, 2000, 38:1713-1740.
12. Poschel T, Schwager T, Brilliantov N V. Rolling friction of a hard cylinder on a viscous plane. *The European Physical Journal B*, 1999, 10:169-174.
13. Qin H. Flow behavior of granular materials: Quasi-static to inertial transition. Thesis of Science Master, The University of Florida, 2000.
14. Sakaguchi, H. Ozaki, E., and Igarashi, T. Plugging of the flow of granular materials during the discharge from a silo. *Journal of Modern Physics B*. 1993, 7:1949-1963.
15. Savage S B, Sayed M. Stresses developed by dry cohesionless granular materials sheared in an annular shear cell. *Journal of Fluid Mechanics*, 1984, 142, 391-430.
16. Staron L, Hinch E J. Study of the collapse of granular columns using two-dimensional discrete-grain simulation. *Journal of Fluid Mechanics*, 2005, 545:1-27.
17. Suiker A S J, Fleck N A. Frictional collapse of granular assemblies. *Transactions of the ASME*, 2004, 71: 350 - 358.
18. Ting J M, Corkum, B T, Kaufman C. R. and Greco C. Discrete numerical modeling for soil mechanics. *J. Geotechnical Engineering*, 1989, 115:379 -398.
19. Zhou Y C, Wright B D, Rang R Y, Xu B H, Yu A B. Rolling friction in the dynamic simulation of sandpile formation. *Physica A*, 1999, 269:536-553.
20. Zhou Y C, Xu B H, Yu A B. Numerical investigation of the angle of repose of monosized spheres. *Physical Review E*, 2001, 64:021301.